Proc. Natl. Acad. Sci. USA
Vol. 86, pp. 5723–5727, August 1989
Biochemistry

Structural characterization of a 2:1 distamycin A·d(CGCAAATTGGC) complex by two-dimensional NMR

(drug–DNA interactions/drug binding/DNA minor groove/intermolecular contacts)

JEFFREY G. PELTON AND DAVID E. WEMMER*

Department of Chemistry, University of California, and Chemical Biodynamics Division, Lawrence Berkeley Laboratory, 1 Cyclotron Road, Berkeley, CA 94720

Communicated by Ignacio Tinoco, Jr., April 28, 1989

ABSTRACT **Two-dimensional NMR has been used to study the 2:1 distamycin A·d(CGCAAATTGGC)·d(GCCAATTTGCG) complex. The nuclear Overhauser effect spectroscopy (NOESY) experiment was used to assign the aromatic and C1′H DNA protons and to identify drug–DNA contacts. These data indicate that two drug molecules bind simultaneously in the minor groove of the central 5′-AAATT-3′ segment and are in close contact with both the DNA and one another. One drug binds with the formyl end close to the second adenine base of the A-rich strand, while the other drug binds with the formyl end close to the second adenine of the complementary strand. With this binding orientation, the positively charged propylamidinium groups are directed toward opposite ends of the helix. Molecular modeling shows that the minor groove must expand relative to the 1:1 complex to accommodate both drugs. Energy calculations suggest that electrostatic interactions, hydrogen bonds, and van der Waals forces contribute to the stability of the complex.**

An understanding of drug–DNA interactions at the molecular level is important in facilitating the design of new drugs and probes that can recognize specific DNA sequences. Distamycin A is an oligopeptide antibiotic (Fig. 1) that binds preferentially to the minor groove of A+T-rich DNA sites (1, 2). Recently, several studies of 1:1 distamycin A·DNA complexes have provided insight into both the specificity and the forces responsible for the tight binding of this drug. Footprinting and affinity cleaving studies (3) have shown that distamycin A binds tightly to 5′-AAATT-3′ in two orientations to a degree dependent on flanking base pairs and, in general, prefers sites that contain several adjacent adenine residues. NMR studies of distamycin A with $d(CGCGAATTCGCG)_2$ (4, 5) have shown that 5′-AATT-3′ is a good binding site, while calorimetric studies of distamycin A with $d(GCGAATTCGC)_2$ (6) indicate that the binding constant for the complex is near $3 \times 10^8\ M^{-1}$, and that the binding process is enthalpy driven. Recent crystallographic studies of distamycin A with $d(CGCAAATTTGCG)_2$ (7) revealed that the drug bound to a 5′-ATTT-3′ sequence, although other sites with four A·T base pairs were available. Similar results have been obtained from footprinting (8, 9), calorimetric (10), crystallographic (11–14), and NMR (15–18) studies of netropsin·DNA complexes. Analysis of these data indicates that van der Waals forces, hydrogen bonds, and electrostatic forces (19) contribute to the stability of these complexes and the sequence specificity of these drugs.

Using NMR spectroscopy, we have now examined the binding of distamycin A to d(CGCAAATTGGC)·d(GCCAATTTGCG),† henceforth called the AAATT duplex. Our major motivation was to examine which binding sites were occupied in solution when a sequence with more than the minimal four A·T base pairs was available. Titration of the DNA with distamycin A showed that at low drug-to-DNA ratios at least two different binding sites were occupied. The binding behavior in this regime will be described elsewhere. At higher amounts of added drug, but still below a 1:1 ratio, a new binding mode was evident; a complex using this mode became the only form present at a drug-to-DNA ratio of 2:1. It is the structure of this 2:1 complex which will be described here. Nuclear Overhauser effect spectroscopy (NOESY) (20) data were used to assign the single set of DNA resonances and identify contacts between the bound drugs and the DNA and also between the two inequivalent drugs in the complex. Distance restraints derived from the NOESY experiment were used with the Assisted Model Building and Energy Refinement (AMBER) (21) molecular mechanics program to develop a model for the complex and to evaluate the contributions to the binding energy.

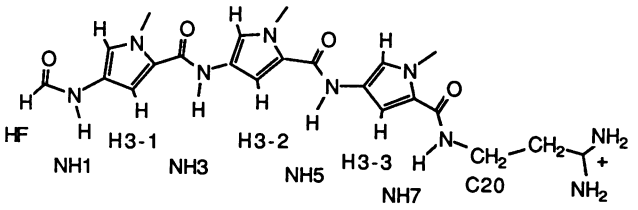

FIG. 1. Schematic of distamycin A. The drug consists of a formyl group, followed by three *N*-methylpyrrole carboxamide units, and a propylamidinium group. The numbering scheme used in this paper is shown.

MATERIALS AND METHODS

Distamycin A was purchased from Sigma and used without further purification. Drug concentrations were calculated by using an extinction coefficient of $34{,}000\ M^{-1}\cdot cm^{-1}$ at 303 nm. Due to the instability of the drug in aqueous solutions, fresh samples were prepared for each titration.

The deoxynucleotides d(CGCAAATTGGC) and d(GCCAATTTGCG) were synthesized by using the phosphite triester method (22, 23) on an Applied Biosystems 381A synthesizer. DNA reagents were purchased from American Bionetics (Hayward, CA). After deprotection by heating overnight at 60°C in 15 M NH_4OH, the dimethoxytrityl (DMT)-containing oligomers were purified by reverse-phase C_{18} chromatography on an IBM LC/9533 ternary gradient chromatograph using a triethylammonium acetate/acetonitrile solvent system. The dimethoxytrityl groups were

The publication costs of this article were defrayed in part by page charge payment. This article must therefore be hereby marked "*advertisement*" in accordance with 18 U.S.C. §1734 solely to indicate this fact.

Abbreviations: NOE, nuclear Overhauser effect; NOESY, nuclear Overhauser effect spectroscopy; D1, drug 1; D2, drug 2.

*To whom reprint requests should be addressed.

†Numbering scheme for the undecamer is strand 1, d(CGCAAATTGGC), residues 1–11, and strand 2, d(GCCAATTTGCG), residues 12–22. Residue 1 is referred to as C1, etc.

cleaved in 80% (vol/vol) acetic acid, then the strands were mixed, annealed, and applied to a hydroxylapatite column (Bio-Rad DNA-grade) to remove excess single strands. The duplex was then dialyzed against 5 mM sodium phosphate, pH 7.0/5 mM sodium chloride. The final sample buffer contained 10 mM sodium phosphate, 10 mM sodium chloride, 1 mM EDTA, and 0.5 mM 2,2,3,3-tetradeutero-3-(trimethylsilyl)propionic acid (TSP) as an internal reference. Extinction coefficients for d(CGCAAATTGGC) and d(GCCAATTTGCG) were calculated (24) to be 1.04×10^5 and 1.01×10^5 $M^{-1} \cdot cm^{-1}$, respectively. Absorbances were determined at 80°C. Double-strand DNA concentrations for samples used in various experiments were 2–4 mM. The purity of the oligomer was greater than 90% as judged on the basis of results of PAGE.

NMR samples were prepared by drying in a Speed Vac concentrator (Savant) and dissolving in 99.96% ^2H_2O (ICN). To observe exchangeable protons the sample was redissolved in 400 μl of a 90:10 (vol/vol) $H_2O/^2H_2O$ solution.

NOESY spectra were acquired on a GN-500 spectrometer (General Electric Instruments) and were processed as described (5). One-dimensional NOE difference spectra of exchangeable protons were acquired by interleaving on- and off-resonance saturated spectra. A 1–3–3–1 pulse sequence (25) was used to suppress the solvent resonance.

RESULTS

DNA and Drug Proton Assignments. Expansions of the aromatic to upfield (1.0 ppm) and aromatic to C1'H regions of a NOESY spectrum of the AAATT duplex taken with two equivalents of added drug are shown in Fig. 2. In the aromatic to C1'H region, cross peaks correlating each DNA aromatic proton (pyrimidine H6 or purine H8) with a C1'H on the same base and with a C1'H proton on the 5' neighboring base were found for both DNA strands, allowing the assignment of these protons by sequential methods (26, 27). These connectivities were confirmed by assignment of the C2'H and C2"H protons. A review of the intensities of these cross peaks did not suggest any striking conformational changes in the AAATT duplex. A more detailed conformational picture would require an analysis of the time dependence of the NOESY cross peaks, which was not attempted in this study. Additional peaks in this region arise from intermolecular contacts (discussed below).

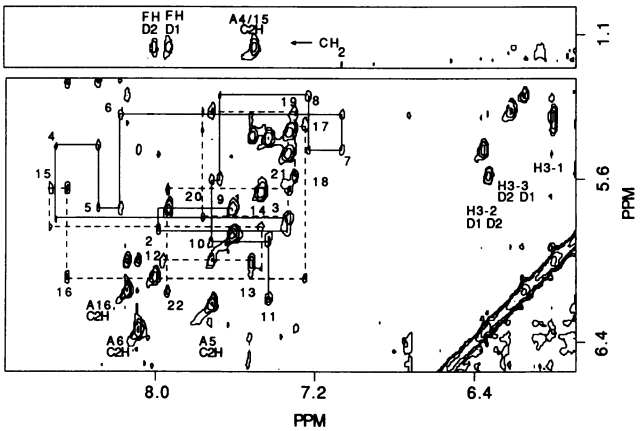

FIG. 2. Expansion of the aromatic to upfield and aromatic to C1'H regions of a NOESY spectrum of the 2:1 distamycin A·d(CGCAAATTGGC) complex (20°C, mixing time 150 ms). The sequential connectivities of the A-rich and T-rich strands are denoted by solid and broken lines, respectively. Intraresidue aromatic to C1'H cross peaks are indicated with numbers. Drug proton and DNA C2H proton positions are explicitly labeled.

Cross peaks in the aromatic to C1'H region of the NOESY spectrum were also used to assign several adenine C2H resonances. In general, for A-rich sequences, NOEs are observed from the C2H of an adenine residue to the C1'H of its 3' neighbor, and to the 3' neighbor of the complementary base (28–31). These are clearly seen in NOESY spectra of the AAATT duplex alone (data not shown). Since A6 and T19 are the 3' neighbor and the 3' neighbor of the complementary base of A5, respectively, the resonance at 7.71 ppm, with cross peaks to A6 and T19 C1'H, must belong to A5 C2H. Another pair of cross peaks connect the resonance at 8.13 ppm with T8 and T17 C1'H, which must therefore belong to A16 C2H. Finally, cross peaks correlate a resonance at 8.07 ppm with T7 C1'H and A5 C2H and must belong to A6 C2H. These assignments were confirmed, and, in addition, the A4 and A15 C2H assignments were determined by systematic one-dimensional NOE experiments of the DNA imino protons (32). The DNA aromatic and C1'H proton assignments are summarized in Table 1.

The origins of the drug H3 pyrrole resonances in the 2:1 complex were determined by first assigning these resonances after addition of a stoichiometric amount of distamycin A. At this point in the titration, two sets of drug resonances appeared (ratio 1.5:1) between 6.3 and 6.7 ppm corresponding to the binding of distamycin A in one of two orientations (33). The drug H3 proton assignments associated with the major binding form were determined through one-dimensional NOEs of the drug amide protons as described (4). The drug H3 proton assignments associated with the minor binding form were then obtained by analysis of chemical exchange cross peaks observed in a NOESY spectrum (20) taken with 0.5 equivalent of added distamycin A (33). These cross peaks occur due to exchange of the drug between the major and minor binding sites, allowing for the direct transfer of the major form assignments to the minor form. These major and minor form assignments were then transferred to the 2:1 complex, in a similar manner, by analysis of chemical exchange cross peaks observed between the 1:1 and 2:1 complexes, in a NOESY spectrum acquired with 1.25 equivalents of added drug. The drug proton assignments are summarized in Table 1.

Intermolecular Contacts. In addition to the intramolecular NOEs used in assignment of DNA resonances, the NOESY spectrum contains many intermolecular (drug–DNA) NOEs, indicating close proximity of specific drug–DNA proton pairs. In Fig. 2 it can be seen that each H3 proton gives a strong NOE to a C1'H proton. Specifically, the chemical shift degenerate H3-1 protons of the two drugs, which will hereafter be referred to as D1 and D2, give NOEs to A6 and T17 C1'H, while the D1 and D2 H3-2 protons give NOEs to T7 and T18 C1'H, respectively, and the D1 and D2 H3-3 protons give NOEs to T8 and T19 C1'H, respectively. Cross peaks also correlate each drug H3 proton with an adenine C2H proton. Specifically, cross peaks correlate the D1 and D2 H3-1 protons with A5 and A16 C2H, the H3-2 drug protons with A6 C2H, and D1 and D2 H3-3 protons with A16 and A5 C2H, respectively. An NOE is observed between H3-1 and A6 C2H, but it is weaker than the other H3-1–C2H cross peaks by a factor of 3, and it may contain contributions from the H3-1 protons of both drugs. Intermolecular NOEs are also observed between two sharp resonances at 7.92 and 7.99 ppm, which can be assigned to the D1 and D2 formyl protons, and A5 and A16 C1'H, respectively.

In the aromatic to upfield region of the NOESY spectrum (Fig. 2), it can be seen that NOEs connect the D1 and D2 formyl protons with a resonance at 1.12 ppm and with resonances at 2.14 and 2.20 ppm, respectively (not shown). Examination of the upfield region of the NOESY spectrum revealed the presence of strong NOEs between the resonance at 1.12 ppm and the resonances at 2.14 and 2.20 ppm.

Table 1. DNA and drug proton resonance assignments in the 2:1 distamycin A·d(CGCAAATTGGC) complex (ppm)

DNA assignments						Drug assignments		
Residue	Aromatic*	C1'H	Residue	Aromatic*	C1'H	Residue	D1	D2
C1	7.61	5.74	G12	7.95	6.00	HF	7.92	7.99
G2	7.97	5.84	C13	7.51	6.06	H3-1	6.00	6.00
C3	7.33	5.80	C14	7.46	5.83	H3-2	6.35	6.33
A4	8.48	5.44	A15	8.53	5.65	H3-3	6.14	6.22
A5	8.28	5.74	A16	8.44	6.08	$\cdot CH_2$	1.12	1.12
A6	8.17	5.28	T17	7.24	5.33		2.14	2.20
T7	7.06	5.45	T18	7.30	5.58			
T8	7.23	5.19	T19	7.30	5.27			
G9	7.67	5.60	G20	7.76	5.78			
G10	7.71	5.89	C21	7.33	5.65			
C11	7.44	6.20	G22	7.94	6.15			

D1 and D2 are drug 1 and drug 2; see text.
*Purine H8 or pyrimidine H6 proton.

Furthermore, the resonance at 1.12 ppm is *J* coupled to these resonances [determined in a correlated spectroscopy (COSY) spectrum, not shown] and to a pair near 3.5 ppm. This pattern is indicative of the D1 and D2 propylamidinium group protons. Thus, the peak at 1.12 ppm contains two C20 methylene resonances, one from each drug, while the peaks at 2.14 and 2.20 ppm correspond to the other C20 protons of D1 and D2, respectively. The cross peaks in the aromatic to upfield region therefore represent intermolecular drug–drug contacts between the formyl and methylene groups. NOEs are also observed between the C20 protons and both A4 and A15 C2H, which are degenerate in chemical shift. A summary of the drug–DNA and drug–drug contacts is given in Table 2.

DISCUSSION

In titrations of the AAATT duplex with distamycin A, resonances associated with the new 2:1 binding mode are observed before a stoichiometry of 1:1 is reached, accounting for approximately 10% of the total at three-quarters of an equivalent of added drug. This indicates that the drug binding affinity in the 2:1 mode is almost as high as in the 1:1 modes. Exchange studies further suggest that the two drugs do not bind as a preformed dimer (details will be presented elsewhere). We have also studied the binding of distamycin A to an oligonucleotide containing the sequence 5'-AAATTT-3', and we find a very similar 2:1 binding mode. However, in this case, the 2:1 complex becomes populated at lower amounts of added drug (below one-half equivalent), indicating an affinity that is essentially the same as in the 1:1 mode.

The precise drug binding sites can be inferred from the intermolecular drug–DNA NOEs. For D1, the H3-1, -2, and -3 pyrrole protons give strong NOEs (and are therefore close) to A5, A6, and A16 C2H and A6, T7, and T8 C1'H protons, respectively. Hence, the D1 pyrrole rings span the A5-A6-T7 sequence, oriented so the formyl proton is near the 5' side of the A-rich strand. NOEs between D1 HF and A5 C1'H and between D1 CH_2 and A15 C2H confirm this binding orientation. Similarly the H3-1, -2, and -3 pyrrole protons of D2 are close to A16, A6, and A5 C2H and T17, T18, and T19 C1'H, respectively. This indicates that the D2 pyrrole rings span the A5-A6-T7 sequence in a manner similar to D1, but with the drug oriented so the formyl proton is near the 5' side of the T-rich strand. NOEs between D2 HF and A16 C1'H, and between D2 CH_2 and A4 C2H confirm the binding orientation of D2. Furthermore, the observed interdrug HF-CH_2 NOEs confirm the positions of D1 and D2 relative to one another. Together, these data indicate that there is a two-drug minor-groove binding site in the central portion of this undecamer, with D1 in close contact with the sequence 5'-AATT-3' of the A-rich strand, and with D2 is in close contact with the sequence 5'-ATTT-3' of the T-rich strand, as indicated in Fig. 3.

Table 2. Intermolecular NOEs observed in the 2:1 complex

NOEs between drug and DNA protons			NOEs between drug protons	
Drug proton	DNA proton correlated with D1	DNA proton correlated with D2	D1 proton	D2 proton
HF	A5 C1'H	A16 C1'H	HF	CH_2
H3-1	A5 C2H	A16 C2H	CH_2	HF
	A6 C1'H	T17 C1'H		
H3-2	A6 C2H	A6 C2H		
	T7 C1'H	T18 C1'H		
H3-3	A16 C2H	A5 C2H		
	T8 C1'H	T19 C1'H		
CH_2	A15 C2H	A4 C2H		

The NMR data also indicate that the sequence and orientational specificity in the 2:1 mode is very high. At low drug-to-DNA ratios, where 1:1 complexes dominate, we have evidence that the drug binds to all four possible binding sites composed of four successive A·T base pairs (unpublished observation). However, we observe only one form of the 2:1 complex. It seems reasonable that the antiparallel orientation of the drugs is favored because it reduces charge–charge repulsion between the positively charged propylamidinium groups. Moreover, of the two possible antiparallel complexes

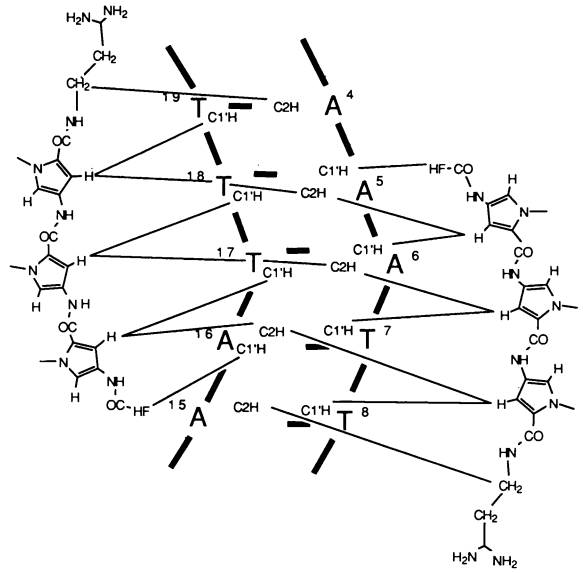

FIG. 3. Schematic of the distamycin A binding sites on d(CGCAAATTGGC). Intermolecular contacts are represented by lines.

(differing by exchange of the drugs across the minor groove), only one is observed, indicating that the drugs are able to "read the walls" of the minor groove in considerable detail. The exact mechanism by which this is accomplished is not yet clear.

Qualitative modeling was carried out with the AMBER molecular mechanics package as described previously for a 1:1 complex (5). For the present calculations the D1 and D2 H3 to C1'H and adenine C2H proton distances were used as constraints. The resulting structure is presented in Fig. 4. In previous studies of distamycin A· and netropsin·DNA complexes, electrostatic interactions, hydrogen bonds, and van der Waals forces have been put forth to account for the large binding energy associated with these drugs. In our model, the charged end of each distamycin A molecule is located deep in the minor groove where the electrostatic potential is large (34), thus contributing favorably to the free energy of complex formation. Hydrogen bonds between the drug amide and A N3 and T O2 atoms also stabilize the complex. For D1 hydrogen bonds are observed between HN1 and A5 N3, HN3 and A6 N3, HN5 and T7 O2, and between HN7 and T8 O2. Analogous hydrogen bonds are observed for D2. Previous studies of 1:1 distamycin A· and netropsin·DNA complexes (5, 7, 11–13) have shown that three-center (35) hydrogen bonds form between the drug amide and A N3 and T O2 atoms on opposite strands of the duplex. Formation of such hydrogen bonds in the 2:1 complex is impossible because the drugs are pushed to the sides of the groove.

Molecular modeling also suggests that the distamycin A molecules are staggered with respect to one another so that the drug pyrrole rings of one drug stack with the amide linkages of the opposing drug on one side, and with DNA sugar O1' atoms on the other side. Staggering also explains the absence of NOEs between H3 protons on opposite drugs. Previous studies of minor-groove binding molecules have shown that they are in complete van der Waals contact with the floor and walls of the minor groove. In particular, stacking interactions were noted between the DNA sugar O1' atoms and the drug aromatic rings (5, 11–14, 36) analogous to those that stabilize Z-DNA (37). These interactions are also present in the 2:1 complex, although altered in detail due to the different positions of the drugs. Thus, in addition to electrostatic forces and hydrogen bond formation, drug–DNA and drug–drug stacking interactions appear to contribute to the stability of the complex.

Recent crystallographic studies have shown the minor groove of A+T-rich sequences to be narrow when compared with ideal B-form DNA (7, 38, 39). For example, the minor-groove width of the A-rich region of d(CGCGAATTCGCG)$_2$ ranged from 3.2 to 4.0 Å (closest phosphate distance less 5.8 Å) (38), compared to the ideal B-form value of 6.0 Å (48). If the thickness of each drug is taken as 3.4 Å, binding two drugs must expand the minor groove to at least 6.8 Å, a value significantly larger than found in the crystal structures of these A-rich sequences. Minor groove widening has also been observed as the result of drug binding to G-C sequences. In an NMR study of the 2:1 actinomycin D·d(ATGCGCAT)$_2$ complex, it was shown that the pentapeptide lactone rings associated with the benzenoid portion of each drug bind simultaneously in the minor groove of the G-rich region of the octamer with concomitant minor groove widening (40). Also, in a recent NMR study of the G-C-specific drug chromomycin (41) it was shown that the drug binds as a dimer to the sequence d(TTGGCCAA)$_2$ and that sugar ring D of one drug and the chromomycinone unit of the other overlap and expand the minor groove. Taken together, our data and that on G-C sequences show that the phosphate backbone of DNA is flexible and that the major- and minor-groove widths of both A+T- and G+C-rich regions can be altered to accommodate binding of other molecules. This conclusion is consistent with the minor-groove widening observed in the *trp* repressor–operator complex (42) and with the major-groove widening observed in the bacteriophage 434 repressor–operator (43) and *Eco*RI endonuclease–DNA complexes (44). Whether this flexibility is sequence dependent and relates to binding specificity remains to be determined. In any case, for the 2:1 mode, it is clear that the intrinsic width (shape) of the minor groove is not a factor in determining such specificity.

The identification of this complex by NMR may have implications for other types of measurements on this class of

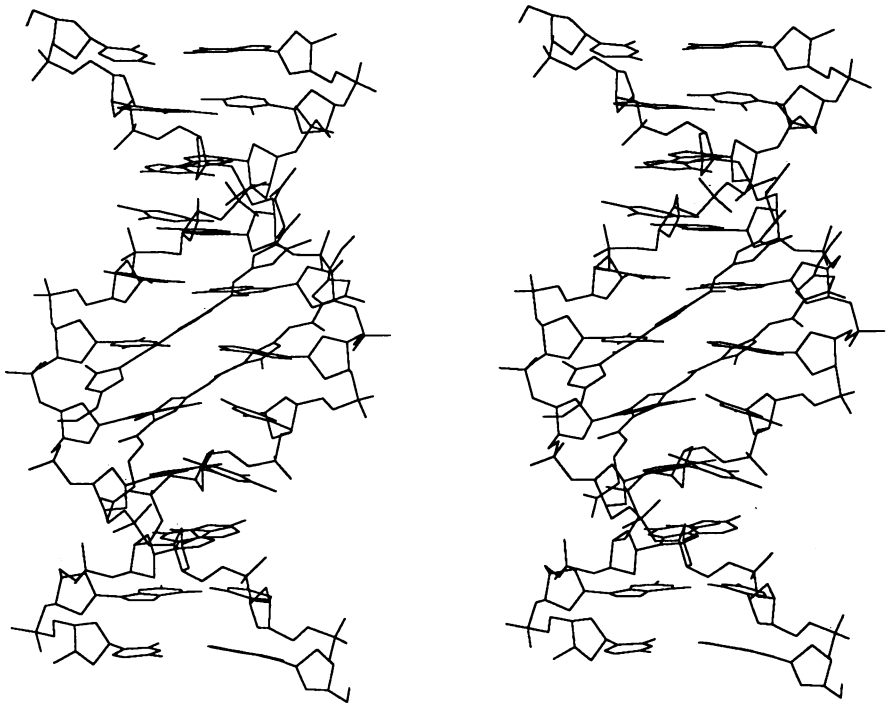

FIG. 4. Stereo drawing of the distamycin A·d(CGCAAATTGGC) complex obtained by energy refinement using semiquantitative distance constraints derived from NOESY.

drug as well. For instance, a considerable amount of work using footprinting and affinity cleaving methods has been reported (3, 45, 46). Since most of this work was performed at very low drug concentrations relative to the number of DNA binding sites, no problems should arise from 2:1 binding. However, some DNase I footprinting work has been conducted at sufficiently high drug-to-DNA ratios that the 2:1 binding mode could be important (9). Moreover, in a recent study of the minor-groove binding drugs (4*S*)- (+)- and (4*R*)- (−)-anthelvencin A, a binding site size of four base pairs was obtained by footprinting methods, but a binding site size of only two base pairs was obtained by optical titration under saturating conditions (47), suggesting that these molecules form a type of 2:1 complex. Since these molecules are charged at both ends, it would seem that formation of a complex similar to that seen here would be destabilized by intermolecular charge–charge repulsion, although formation of a highly staggered complex might be investigated. Data obtained by other methods which utilize high drug-to-DNA ratios (such as calorimetry) are most likely to be affected. From the limited information now available, it is easier to form the 2:1 complex with larger A-rich sequences (AATT << AAATT < AAATTT). Whether distamycin A binding to polymers such as $d(A)_n \cdot d(T)_n$ and $d(AT)_n$ might occur preferentially in the 2:1 mode is, as yet, unclear.

The structure of this complex, including both the sequence and orientational specificity, also suggests a strategy for the design of new drugs and probes. In fact, it may be possible to combine recognition of one strand of the DNA with specific interactions between two drug molecules (or another part of the same drug molecule), to create a sequence-specific recognition complex. Interactions that stabilize the present 2:1 mode, and which should be used as a guide in the design of such drugs, include drug–drug and drug–DNA stacking, hydrogen bonding, and electrostatic forces.

We greatly appreciate an initial collaboration with Prof. R. Klevit, and we thank D. Koh for help with DNA synthesis. This work was supported by the National Institutes of Health through the University of California Berkeley Biological Research Support Grant Program, the Office of Energy Research, Health Effects Research Division of the U.S. Department of Energy, Contract DE AC03 76SF00098, and equipment grants from the Department of Energy University Research Instrumentation Program (DE F605 86ER75281) and the National Science Foundation (DMB 8609035).

1. Hahn, F. E. (1975) in *Antibiotics III: Mechanism of Action of Antimicrobial and Antitumor Agents*, eds. Corcoran, J. W. & Hahn, F. E. (Springer, New York), pp. 79–100.
2. Zimmer, C. & Wahnert, U. (1986) *Prog. Biophys. Mol. Biol.* **47**, 31–112.
3. Schultz, P. G. & Dervan, P. B. (1984) *J. Biomol. Struct. Dyn.* **1**, 1133–1147.
4. Klevit, R. E., Wemmer, D. E. & Reid, B. R. (1986) *Biochemistry* **25**, 3296–3303.
5. Pelton, J. G. & Wemmer, D. E. (1988) *Biochemistry* **27**, 8088–8096.
6. Breslauer, K. J., Remeta, D. P., Chou, W.-Y., Ferrante, R., Curry, J., Zaunczkowski, D., Snyder, J. G. & Marky, L. A. (1987) *Proc. Natl. Acad. Sci. USA* **84**, 8922–8926.
7. Coll, M., Frederick, C. A., Wang, A. H.-J. & Rich, A. (1987) *Proc. Natl. Acad. Sci. USA* **84**, 8385–8389.
8. Ward, B., Rehfuss, R., Goodisman, J. & Dabrowiak, J. C. (1988) *Biochemistry* **27**, 1198–1205.
9. Fish, L., Lane, M. J. & Vournakis, J. N. (1988) *Biochemistry* **27**, 6026–6032.
10. Marky, L. A., Blumenfeld, K. S. & Breslauer, K. J. (1983) *Nucleic Acids Res.* **11**, 2857–2870.
11. Kopka, M. L., Yoon, C., Goodsell, D., Pjura, P. & Dickerson, R. E. (1985) *Proc. Natl. Acad. Sci. USA* **82**, 1376–1380.
12. Kopka, M. L., Yoon, C., Goodsell, D., Pjura, P. & Dickerson, R. E. (1985) *J. Mol. Biol.* **183**, 553–563.
13. Kopka, M. L., Pjura, P., Yoon, C., Goodsell, D. & Dickerson, R. E. (1985) in *Structure and Motion: Membranes, Nucleic Acids, and Proteins*, eds. Clementi, E., Corongiu, G., Sarma, M. H. & Sarma, R. H. (Adenine Press, New York), pp. 461–483.
14. Coll, M., Aymami, J., van der Marel, G. A., van Boom, J. H., Rich, A. & Wang, A. J. (1989) *Biochemistry* **28**, 310–320.
15. Patel, D. J. (1982) *Proc. Natl. Acad. Sci. USA* **79**, 6424–6428.
16. Patel, D. J. & Shapiro, L. (1985) *Biochimie* **67**, 887–915.
17. Sarma, M. H., Gupta, G. & Sarma, R. H. (1985) *J. Biomol. Struct. Dyn.* **2**, 1085–1095.
18. Pardi, A., Morden, D. M., Patel, D. J. & Tinoco, I. (1983) *J. Am. Chem. Soc.* **22**, 1107–1113.
19. Lavery, R., Zakrzewska, K. & Pullman, B. (1986) *J. Biomol. Struct. Dyn.* **3**, 1155–1170.
20. Jeener, J., Meier, B. H., Bachmann, P. & Ernst, R. R. (1979) *J. Chem. Phys.* **71**, 4546–4553.
21. Weiner, S. J., Kollman, P. A., Case, D. A., Singh, U. C., Ghio, C., Alagona, G., Profeta, S., Jr., & Weiner, P. (1984) *J. Am. Chem. Soc.* **106**, 765–784.
22. Letsinger, R. L. & Lunsford, W. B. (1976) *J. Am. Chem. Soc.* **98**, 3655–3661.
23. Matteucci, M. D. & Caruthers, M. H. (1981) *J. Am. Chem. Soc.* **103**, 3185–3191.
24. Warshaw, M. & Cantor, C. (1970) *Biopolymers* **9**, 1079–1103.
25. Hore, P. J. (1983) *J. Magn. Reson.* **55**, 283–300.
26. Scheek, R. M., Boelens, R., Russo, W., van Boom, J. H. & Kaptein, R. (1984) *Biochemistry* **23**, 1371–1376.
27. Hare, D. R., Wemmer, D. E., Chou, S.-H., Drobny, G. & Reid, B. R. (1983) *J. Mol. Biol.* **171**, 319–336.
28. Patel, D. J., Shapiro, L., Kozlowski, S. A., Gaffney, B. L. & Jones, R. A. (1986) *J. Mol. Biol.* **188**, 677–692.
29. Weiss, M. A., Patel, D. J., Sauer, R. T. & Karplus, M. (1984) *Nucleic Acids Res.* **12**, 4035–4047.
30. Behling, R. W. & Kearns, D. R. (1986) *Biochemistry* **25**, 3335–3346.
31. Kintanar, A., Klevit, R. E. & Reid, B. R. (1987) *Nucleic Acids Res.* **15**, 5845–5862.
32. Chou, S.-H., Hare, D. R., Wemmer, D. E. & Reid, B. R. (1983) *Biochemistry* **22**, 3037–3041.
33. Pelton, J. G. & Wemmer, D. E. (1989) in *Frontiers of NMR in Molecular Biology, UCLA Symposia on Molecular and Cellular Biology: New Series*, eds. Live, D., Armitage, I. & Patel, D. (Liss, New York), in press.
34. Lavery, R., Pullman, A. & Pullman, B. (1982) *Theor. Chim. Acta* **62**, 93–106.
35. Taylor, R., Kennard, O. & Werner, V. W. (1984) *J. Am. Chem. Soc.* **106**, 244–248.
36. Teng, M.-K., Usman, N., Frederick, C. A. & Wang, A. H.-J. (1988) *Nucleic Acids Res.* **16**, 2671–2690.
37. Wang, A. H.-J., Quigley, G. J., Kolpak, F. J., Crawford, J. L., van Boom, J. H., van der Marel, G. & Rich, A. (1979) *Nature (London)* **282**, 680–686.
38. Fratini, A. V., Kopka, M. L., Drew, H. R. & Dickerson, R. E. (1982) *J. Biol. Chem.* **256**, 14686–14707.
39. Nelson, H. C. M., Finch, J. T., Luisi, B. F. & Klug, A. (1987) *Nature (London)* **330**, 221–226.
40. Scott, E. V., Zon, G., Marzilli, L. G. & Wilson, W. D. (1988) *Biochemistry* **27**, 7940–7951.
41. Gao, X. & Patel, D. J. (1989) *Biochemistry* **28**, 751–762.
42. Otwinowski, Z., Schevitz, R. W., Zhang, R.-G., Lawson, C. L., Joachimiak, A., Marmorstein, R. Q., Luisi, B. R. & Sigler, P. B. (1988) *Nature (London)* **335**, 321–329.
43. Anderson, J. E., Ptashne, M. & Harrison, S. C. (1987) *Nature (London)* **326**, 846–852.
44. McClarin, J. A., Frederick, C. A., Wang, B.-C., Greene, P., Boyer, H. W., Grable, J. & Rosenberg, J. M. (1986) *Science* **234**, 1526–1541.
45. Schultz, P. G. & Dervan, P. B. (1983) *J. Am. Chem. Soc.* **105**, 7748–7750.
46. Taylor, J. S., Schultz, P. G. & Dervan, P. B. (1984) *Tetrahedron* **40**, 457–465.
47. Lee, M., Shea, R. G., Hartley, S. A., Kissinger, K., Pon, R. T., Vesnaver, G., Breslauer, K. J., Dabrowiak, J. C. & Lown, J. W. (1989) *J. Am. Chem. Soc.* **111**, 345–354.
48. Chandrasekaran, R. & Arnott, S. (1989) *Landolt-Börnstein Numerical Data and Functional Relationships*, ed. Saenger, W. (Springer, New York), Vol VII/16, pp. 30–170.